

# Effect of cepharanthine on the stemness of lung squamous cell carcinoma based on network pharmacology and bioinformatics

Bo Liu

Department of Oncology, Pingxiang Second People's Hospital

Jian-xiong Deng (✉ [djx1012@126.com](mailto:djx1012@126.com))

Department of Oncology, Gaoxin Hospital of the First Affiliated Hospital of Nanchang University

---

## Research Article

**Keywords:** Cepharanthine, Lung squamous cell carcinoma, Stemness, Immune infiltration, Network Pharmacology, Bioinformatics

**Posted Date:** June 15th, 2022

**DOI:** <https://doi.org/10.21203/rs.3.rs-1739051/v1>

**License:**   This work is licensed under a Creative Commons Attribution 4.0 International License.

[Read Full License](#)

---

# Abstract

**Background.** Lung squamous cell carcinoma (LUSC) has poor survival prognosis and few clinical treatment options. We urgently need to explore new therapeutic drugs in clinical practice. Cepharanthine (CEP), which has been shown to have anticancer effects in several tumors, but the mechanism of CEP in treating LUSC has not been reported.

**Methods.** SwissTargetPrediction, PharmMapper and GeneCards were used to identify targets of CEP and LUSC. Further topological analysis was used to obtain hub genes via Cytoscape. Molecular docking was carried out to verify the combination of CEP with hub targets. Based on bioinformatics, we first analyzed the expression and survival of hub targets in LUSC, and further analyzed the correlation between hub targets and cancer stemness, immune cell infiltration and tumor mutation burden (TMB).

**Results.** A total of 41 targets were identified. Further topological analysis identified 6 hub genes: AURKA, CCNA2, CCNE1, CDK1, CHEK1 and PLK1. Molecular docking analysis showed that CEP had stable binding to all these 6 target proteins. In-depth bioinformatics analysis of these 6 targets showed that high expression of these targets were positively correlated with cancer stemness index, and negatively correlated with tumor infiltrating immune cells. In immune subtype analysis, the expressions of these targets were significantly decreased in inflammatory tumors. In addition, we also found that the expressions of these targets were positively correlated with TMB.

**Conclusion.** Based on multidisciplinary analysis, we preliminarily identified potential targets of CEP for LUSC treatment and suggested that CEP may play a role in regulating LUSC stemness.

## Introduction

Lung cancer is the malignant tumor with the highest morbidity and mortality in the world. In 2020, up to 1,796,144 people died of lung cancer worldwide, accounting for 18% of cancer-related deaths[1]. Lung squamous cell carcinoma (LUSC) is a common subtype of lung cancer, accounting for about 25–30% of lung cancer. Almost 50% of LUSC patients have metastases at diagnosis[2]. Despite rapid advances of immunotherapy in recent years, the 5-year survival rate for LUSC stage III and IV disease is only 13% and 2%, respectively[3, 4]. Therefore, there is an urgent need for novel anticancer drugs that mediate the molecular mechanisms underlying LUSC progression.

With the development of Traditional Chinese medicine, its monomer components have become the focus of current scientific research. In the current Novel Coronavirus epidemic, cepharanthine (CEP) has been found to reverse endoplasmic reticulum stress and heat shock response induced by Novel Coronavirus[5]. The anti-Novel Coronavirus effect of CEP was also confirmed in the studies of Ohashi et al[6] and Zhang et al[7]. CEP is a kind of isoquinoline alkaloid extracted from Traditional Chinese medicine *Stephania epigaea* Lo[8]. Previous studies have confirmed that CEP has a variety of pharmacological properties, such as antioxidant, plasma membrane stabilization, anti-inflammatory and immune regulation[9–12]. In the study of tumor mechanism, CEP has been found to inhibit tumor cell proliferation, migration and anti-

angiogenesis. Gao et al.[13] found that CEP may induce apoptosis and autophagy of breast cancer cells through the AKT/mTOR signaling pathway. Uthaisar et al.[14] demonstrated that CEP inhibits the invasion and metastasis of cholangiocarcinoma by inhibiting ICAM-1 and MMP-2. In studies of lung adenocarcinoma, CEP can activate the P38 pathway in A549 cells to regulate autophagy and thus inhibit the malignant biological behavior of A549 cells[15]. However, the study of CEP in LUSC has not been reported.

Network pharmacology, developed by Hopkins et al.[16], seeks to explore the multi-level interactions of disease, genes, and drugs, and based on systems biology, computational biology and omics theory to evaluate the therapeutic effect of Traditional Chinese medicine on diseases. This study aims to explore the molecular mechanism of CEP in the treatment of LUSC through network pharmacology, bioinformatics and molecular docking. Firstly, the protein targets and disease targets of LUSC were predicted and integrated through databases of network pharmacology. Then, functional enrichment analysis was performed for the above target genes, and the protein interaction network diagram was constructed to screen the key targets based on topological analysis. And molecular docking was used to verify the binding of CEP to target protein. To further explore the mechanism of CEP in treating LUSC, we conducted in-depth bioinformatics analysis. It mainly includes the correlation between target and cancer stemness, tumor microenvironment and tumor mutation burden.

## **Materials And Methods**

### **Screening of physicochemical parameters and potential targets of CEP**

TCMSP database[17] was used to obtain characteristic information and physicochemical parameters of CEP. PubChem database (<https://pubchem.ncbi.nlm.nih.gov/>) to obtain the CEP element three-dimensional SDF files and SMELL, The SDF file and import the SMELL.

SwissTargetPrediction[18] website (<http://www.swisstargetprediction.ch/>) and PharmMapper[19] database (<http://lilab-ecust.cn/pharmMapper/>) was used to predict the target sites, and the results of the two databases were combined to obtain the potential target sites of CEP.

### **Potential targets and differential expressed gene analysis of LUSC**

As the "Lung squamous cell carcinoma" as keywords from GeneCards database (<https://www.genecards.org/>) retrieval LUSC of the related targets. RNAseq data (level 3) and corresponding clinical information of LUSC were obtained from the cancer genome atlas (TCGA) dataset (<https://portal.gdc.com>). Differential expression of mRNA was analyzed using "Limma"[20] package of R project. Adjusted P values were analyzed in TCGA or GTEx to correct for false positive results. Adjusted P < 0.05 and  $\log_2$  (Fold Change) > 1 was defined as the threshold for the screening of mRNA differential expression and the mapping of volcano.

### **Construct protein-protein interactions and drug-target-disease networks**

The potential targets of LUSC, differential expressed genes and predicted targets of CEP were intersected to obtain common targets of drugs and diseases, and a Venn diagram was drawn. A protein-protein interaction (PPI) network of common targets was constructed using STRING 11.5 (<https://string-db.org/>) database with a minimum interaction score of 0.4. Cytoscape[21] software was used for visualization. In addition, cytohubba plug-in was used to screen key genes.

### **Functional enrichment analysis**

Gene ontology (GO) is a widely used tool for annotating functional genes, particularly molecular functions (MF), biological pathways (BP), and cellular components (CC). KEGG enrichment analysis is useful for analyzing gene function and related high-level genomic function information. ClusterProfiler[22] package in R project was used to analyze the GO function and KEGG pathway involved in potential targets.

### **Molecular docking analysis**

Molecular docking is a validation method that uses a computer to simulate the binding of receptors and ligands and predict their affinity. PDB format files of target proteins were obtained from RCSB PDB database (<https://www.rcsb.org/>), and AutoDock Tools[23] were used for dehydrating, hydrogenation and charge treatment of target proteins. The file in mol2 format was downloaded from TCMSP[17] database for structural processing. AutoDock Vina[24] was used for molecular docking to calculate binding energy and the best binding conformation. The docking results were visualized using PyMOL (The PyMOL Molecular Graphics System, Version 2.0 Schrodinger, LLC.).

### **Analysis of expression and survival**

Using the RNA-seq data of LUSC in TCGA, R project was used to analyze the differential expression of target genes in normal tissues and tumor tissues, the statistical difference of two groups was compared through the Wilcoxon test. We obtained the gene expression matrix of LUSC cell line from the CCLE database (<https://portals.broadinstitute.org/ccle/about>), and visualized it using heat maps. We retrieved the target genes in The Human Protein Atlas database (<https://www.proteinatlas.org/>), immunohistochemical images were used to directly compare the protein expression of target genes in LUSC and normal lung tissues. Log-rank test was used to compare differences in survival between these groups. For Kaplan-Meier curves, p-values and hazard ratio (HR) with 95% confidence interval (CI) were generated by log-rank tests and univariate cox proportional hazards regression.  $P < 0.05$  was considered statistically significant.

### **The stemness index based on mRNA expression**

Use the one-class logistic regression (OCLR) machine learning algorithm to calculate mRNAsi which constructed by Malta et al.[25]. Based on the mRNA expression signature, the gene expression profile contains 11,774 genes. The minimum value was subtracted, and the result was divided by the maximum

maps the stemness index to the range [0,1]. The closer mRNAsi was to 1, the stronger was the characteristics of stem cells.

## **Tumor immune cells infiltration and tumor mutation burden**

For reliable immune score evaluation, RNA-seq data of LUSC from TCGA database were obtained, and the correlation between target genes and immune cell infiltration was analyzed by TIMER[26] algorithm. Wilcoxon rank-sum test was used to accurately assess the differences in the expression levels of different target genes and the density of immune cell invasion in LUSC. The correlations between targets expression and immune or molecular subtypes of LUSC were explored via the TISIDB[27] database (<http://cis.hku.hk/TISIDB/index.php>). Differences with a P value < 0.05 were considered to be statistically significant. Correlation analysis between target genes expression and TMB was performed using Spearman's method. The above analysis results were visualized by R package ggplot2 and Pheatmap.

# **Results**

## **Common targets of CEP and LUSC**

Through PubChem database, we obtained the 3D structure of CEP (Figure 1a), and predicted 231 and 121 CEP related target proteins by PharmMapper and SwissTargetPrediction databases, respectively. After removing repeated targets, a total of 322 related target genes of CEP were collected (Table S1). 7947 LUSC-related target genes were retrieved from GeneCards database (Table S2). In addition, RNA-seq data of 501 LUSC samples and 49 para-cancer samples from TCGA database and sequencing data of 578 normal lung tissue samples from GTEx database were downloaded to obtain 2194 up-regulated genes in tumor tissues by difference analysis (Figure 1b). Finally, through the intersection of the three gene sets, 41 potential targets for the regulation of LUSC progression were obtained (Figure 1c), and drug-target-disease network was drawn (Figure 1d).

## **Interaction and enrichment analysis of target proteins**

In order to study the correlation between CEP and LUSC, a 41 nodes and 130 edges protein-protein interaction (PPI) network was constructed using String database (Figure 2a). To further define key target proteins in PPI network, the MCC, Degree, DMNC, MNC and Closeness algorithms in CytoHubba plugin are used to calculate node topology parameters (Table S3), and the top 10 targets are selected to intersect. Finally, we get six key target proteins: AURKA, CCNA2, CCNE1, CDK1, CHEK1, PLK1 (Figure 2b). In addition, we also conducted functional enrichment analysis of the GO and KEGG pathways involved in these targets using the R package "ClusterProfile". GO enrichment analysis consisted of three items, biological process (BP), cellular composition (CC) and molecular function (MF). Biological processes mainly involve: negative regulation of apoptotic process, collagen catabolic process, extracellular matrix disassembly, et al. Cellular composition mainly involve: cytosol, extracellular exosome, cyclin-dependent protein kinase holoenzyme complex, et al. And molecular function mainly involve: protein serine/threonine/tyrosine kinase activity, protein kinase activity,

endopeptidase activity, et al (Figure 2c). The KEGG pathway they involved mainly includes: Pathways in cancer, IL-17 signaling pathway, Progesterone-mediated oocyte maturation, Cell cycle, Cellular senescence, p53 signaling pathway, et al (Figure 2d).

## **Molecular docking**

After identifying the 6 key target proteins, we further verified the interaction between CEP and these target proteins by molecular docking. As shown in Table 1, the lowest binding affinity of CEP with AURKA, CCNA2, CCNE1, CDK1, CHEK1 and PLK1 were -9.1 kcal/mol, -8.4 kcal/mol, -9.0 kcal/mol, -9.2 kcal/mol, -7.6 kcal/mol and -8.5 kcal/mol, respectively. The above all show a strong binding affinity. As shown in Figure 3, the binding of CEP with 1mq4 (AURKA) is mainly through the hydrophobic interaction with LYS-143, PHE-144, and GLU-260, hydrogen bonding with amino acid residues LYS-143, LYS-162, LYS-258, and TRP-277, and salt bridge with GLU-260. The binding of CEP with 1fin (CCNA2) is mainly through the hydrophobic interaction with ILE-182, GLN-313, and THR-316, hydrogen bonding with amino acid residues ASN-173, and salt bridge with GLU-268. The binding of CEP with 1w98 (CCNE1) is mainly through the hydrophobic interaction with GLN-240, hydrogen bonding with amino acid residues ASN-236. The binding of CEP with 4y72 (CDK1) is mainly through the hydrophobic interaction with VAL-227, ILE-269, TYR-71 and LYS-274, hydrogen bonding with amino acid residues TYR-270. The binding of CEP with 1ia8 (CHEK1) is mainly through the hydrophobic interaction with GLU-33, and ALA-34, Hydrogen bonding with amino acid residues TYR-71 and TYR-86, and salt bridge with ASP-139 and GLU-140. The binding of CEP with 1q4o (PLK4) is mainly through the hydrophobic interaction with LYS-420, ASP-438, and LYS-474, Hydrogen bonding with amino acid residues ARG-456, and salt bridge with ASP-438 (Table S3).

## **Expression levels of these targets**

To further explore the mechanism of CEP in LUSC, we performed bioinformatics analysis on these 6 key targets. First, we analyzed TCGA transcriptional data and found that they were significantly up-regulated in LUSC tissue compared to normal lung tissue (all  $P < 0.05$ ) (Figure 4a). In the meanwhile, we analyzed the expression data of cell lines in the CCLE dataset and found that these 6 genes were also expressed differently in various cell lines of LUSC (Figure 4b). In addition, we analyzed the HPA database and found that compared with normal lung tissues, the protein expression levels of AURKA, CCNA2, CCNE1, CDK1 and PLK1 were significantly increased in LUSC tissues (Figure 4c-g). The expression of CHEK1 protein has not been recorded in HPA database, but in Grabauskienė's study, CHEK1 protein was upregulated in LUSC[28]. In the analysis of the expression of these targets and survival, the high expression of CCNA2 and CHEK1 was associated with shorter overall survival in LUSC patients ( $P < 0.05$ ), while the other gene expression levels were not significantly associated with overall survival in LUSC patients ( $P > 0.05$ ) (Figure 5).

## **Evaluation of stemness index**

To evaluate the possible effect of CEP on cancer stemness, we divided LUSC samples from TCGA into high expression group and low expression group according to the mRNA expression median value of

target genes. OCLR machine learning algorithm was used to calculate stemness index (mRNAsi) to analyze the stemness degree among samples with differential expression of CEP targets. The results showed that the mRNAsi in the samples with high mRNA expression of AURKA, CCNA2, CCNE1, CDK1, CHEK1 and PLK1 was significantly higher than that in the samples with low mRNA expression (Figure 6).

### **Immune cell infiltration analysis of targets**

Cancer stem cells have been proven to have immunosuppressive effects, and previous studies have shown that CEP has immunomodulatory effects. Therefore, we analyzed the relationship between expression of CEP targets and level of immune cell infiltration in LUSC. By calculating levels of immune cell infiltration for six types, the expression of AURKA were negatively correlated with infiltration levels of B cell, CD4+ T cell, CD8+ T cell, Neutrophil, Macrophage, Myeloid dendritic cell. Similarly, the expression of other target genes is also negatively correlated with the level of immune cell infiltration (Figure 7). Further, we analyzed the relationship between immune subtypes and expression of targets, and immune subtypes were classified into six types, including C1 (wound healing), C2 (IFN-gamma dominant), C3 (inflammatory), C4 (lymphocyte depleted), C5 (immunologically quiet) and C6 (TGF-b dominant). The results showed that AURKA was low expressed in inflammatory samples, while AURKA was high expressed in lymphocyte depleted samples. The correlation between immune subtypes and expression of the other five targets showed similar results (Figure 8).

### **Tumor mutation burden analysis**

Antitumor immunity requires T cells to recognize neoantigens caused by somatic mutations. Therefore, we analyzed the correlation between tumor mutation burden and the expression of targets, and the results showed that the expression of AURKA, CCNA2, CCNE1, CDK1, CHEK1, and PLK1 were significantly positively correlated with the tumor mutation burden (Figure 9).

## **Discussion**

Network pharmacology can explore the complex mechanisms among biological systems, diseases and drugs from the perspective of network, and become an effective method for drug discovery[29]. In addition, molecular docking can accelerate drug design and screening by predicting the affinity and binding pattern between drugs and proteins, and provide a basic theory for future experiments[30]. In this study, a reverse approach based on molecular docking was used to predict CEP targets and integrate them with LUSC targets. A total of 41 candidate targets were identified. The PPI network analysis revealed that CEP may have pharmacological effects on LUSC through 41 candidate targets.

According to the biological processes in GO analysis, 41 candidate targets were found to be related to negative regulation of apoptotic process. Previous studies have shown that CEP can induce apoptosis of myeloma cells by activating caspase-3 pathway[31]. It has also been confirmed that CEP can inhibit the expression of STAT3 gene and lead to the apoptosis of SaOS2 cells[32]. In addition, KEGG analysis showed that the targets of CEP was enriched in pathways in cancer, IL-17 signaling Pathway, Cell cycle,

Cellular senescence, p53 signaling pathway. Previous studies have demonstrated the role of CEP in the treatment of a variety of tumors[33–35], as well as its inhibitory effect on lung cancer cells[36]. However, the mechanism of CEP in treating LUSC has not been reported.

In order to clarify the possible mechanism of CEP in the treatment LUSC, we conducted further research from the perspective of bioinformatics. Six hub genes were identified as AURKA, CCNA2, CCNE1, CDK1, CHEK1 and PLK1 by topological analysis of the 41 targets PPI network. Meanwhile, molecular docking analysis showed that CEP could stably bind these targets.

After determining that CEP can interact with these targets, we further analyzed the role of these targets in LUSC. First of all, we found that the stemness index (mRNAsi) was significantly higher in the samples with high expression of 6 targets than in the samples with low expression. Stemness refers to the cell's self-renewal and differentiation potential[25]. In tumor tissue, there is a group of cells with stem cell-like characteristics called cancer stem cells (CSCs)[37]. mRNAsi index is a new dryness index used to evaluate the dedifferentiation potential of tumor cells. The higher the stemness index, the higher the ability of cancer cells to dedifferentiate[25, 38]. These undifferentiated cancer cells are more likely to metastasize, leading to disease progression and poor prognosis. It also has a significant impact on treatment resistance and immunotherapy response[39]. Therefore, we hypothesized that CEP may inhibit LUSC progression by reducing tumor stemness by acting on these targets.

In addition, we found that the expression of AURKA, CCNA2, CCNE1, CDK1, CHEK1 and PLK1 were all positively correlated with TMB, which was consistent with previous research results, and there was a positive correlation between tumor dryness and tumor mutation burden[38]. It is also consistent with studies demonstrating accumulation of mutations in normal adult stem cells[40].

In terms of immune microenvironment, we found that the expressions of AURKA, CCNA2, CCNE1, CDK1, CHEK1 and PLK1 were negatively correlated with tumor immune infiltrating cells. Meanwhile, we also found that the expression of targets in immune inflammatory tumors was low, and the samples with high expression of targets were mainly distributed in lymphocytes depleted type tumors. Previous studies have shown that in colorectal cancer, lung cancer and ovarian cancer, tumor stemness is negatively correlated with immune cell infiltration, and the higher the stemness of the tumor, the lower the T cell infiltrating level[38].

There are some limitations to this study. We have only explored the role of CEP in LUSC at the level of network pharmacology and bioinformatics, and further studies in molecular biology are needed. Secondly, network pharmacology studies rely more on various existing databases, but the screening criteria for drugs in the databases may not be accurate enough.

In conclusion, our study systematically explored the molecular and pharmacological mechanisms of CEP on LUSC. Six genes were identified as anticancer targets of CEP that reduce LUSC stem cell characteristics and increase immune cell infiltration. This study provides new ideas for treating LUSC and lays a foundation for drug development.

# Declarations

## Acknowledgments

We acknowledge the TCMSP, SwissTargetPrediction, PharmMapper, TCGA, GTEx, HPA and TISIDB databases for free use.

## Funding

The authors declare that no funds, grants, or other support were received during the preparation of this manuscript.

## Competing Interests

The authors have no relevant financial or non-financial interests to disclose.

## Author Contributions

Bo Liu: Conceptualization, Formal analysis and investigation, Writing-original draft preparation. Jian-xiong Deng: Conceptualization, Methodology, Writing-review and editing, Supervision.

## Data Availability

All data is available under reasonable request.

## Ethics approval

This article is not involved in any studies with human participants or animals performed by any of the authors.

## Consent to participate

Not applicable.

## Consent to publication

All authors consent to the publication of this study.

# References

1. Sung H, Ferlay J, Siegel RL, Laversanne M, Soerjomataram I, Jemal A, Bray F (2021) Global Cancer Statistics 2020: GLOBOCAN Estimates of Incidence and Mortality Worldwide for 36 Cancers in 185 Countries. *CA Cancer J Clin* 71(3):209–249
2. Cheung CHY, Juan HF (2017) Quantitative proteomics in lung cancer. *J Biomed Sci* 24(1):37

3. Wang BY, Huang JY, Chen HC, Lin CH, Lin SH, Hung WH, Cheng YF (2020) The comparison between adenocarcinoma and squamous cell carcinoma in lung cancer patients. *J Cancer Res Clin Oncol* 146(1):43–52
4. Nadal E, Massuti B, Domine M, Garcia-Campelo R, Cobo M, Felip E (2019) Immunotherapy with checkpoint inhibitors in non-small cell lung cancer: insights from long-term survivors. *Cancer Immunol Immunother* 68(3):341–352
5. Li S, Liu W, Chen Y, Wang L, An W, An X, Song L, Tong Y, Fan H, Lu C (2021) Transcriptome analysis of cepharanthine against a SARS-CoV-2-related coronavirus. *Brief Bioinform* 22(2):1378–1386
6. Ohashi H, Watashi K, Saso W, Shionoya K, Iwanami S, Hirokawa T, Shirai T, Kanaya S, Ito Y, Kim KS, Nomura T, Suzuki T, Nishioka K, Ando S, Ejima K, Koizumi Y, Tanaka T, Aoki S, Kuramochi K, Suzuki T, Hashiguchi T, Maenaka K, Matano T, Muramatsu M, Saijo M, Aihara K, Iwami S, Takeda M, McKeating JA, Wakita T (2021) Potential anti-COVID-19 agents, cepharanthine and nelfinavir, and their usage for combination treatment. *iScience* 24(4):102367
7. Zhang S, Huang W, Ren L, Ju X, Gong M, Rao J, Sun L, Li P, Ding Q, Wang J, Zhang QC (2022) Comparison of viral RNA-host protein interactomes across pathogenic RNA viruses informs rapid antiviral drug discovery for SARS-CoV-2. *Cell Res* 32(1):9–23
8. Semwal DK, Badoni R, Semwal R, Kothiyal SK, Singh GJ, Rawat U (2010) The genus *Stephania* (Menispermaceae): chemical and pharmacological perspectives. *J Ethnopharmacol* 132(2):369–383
9. Kogure K, Tsuchiya K, Abe K, Akasu M, Tamaki T, Fukuzawa K, Terada H (2003) Direct radical scavenging by the bisbenzylisoquinoline alkaloid cepharanthine. *Biochim Biophys Acta* 1622(1):1–5
10. Shinoda K, Adachi I, Ueno M, Horikoshi I (1990) [Effects of cepharanthine on liposomal permeability and size]. *Yakugaku Zasshi* 110(3):186–190
11. Aota K, Yamanoi T, Kani K, Azuma M (2018) Cepharanthine Inhibits IFN-gamma-Induced CXCL10 by Suppressing the JAK2/STAT1 Signal Pathway in Human Salivary Gland Ductal Cells. *Inflammation* 41(1):50–58
12. Yamazaki T, Shibuya A, Ishii S, Miura N, Ohtake A, Sasaki N, Araki R, Ota Y, Fujiwara M, Miyajima Y, Uetake K, Hamahata K, Kato K, Kawakami K, Toyoda H, Moriguchi N, Okada M, Nishi M, Ogata Y, Takimoto T, Ohga S, Ohta S, Amemiya S (2017) High-dose Cepharanthin for pediatric chronic immune thrombocytopenia in Japan. *Pediatr Int* 59(3):303–308
13. Gao S, Li X, Ding X, Qi W, Yang Q (2017) Cepharanthine Induces Autophagy, Apoptosis and Cell Cycle Arrest in Breast Cancer Cells. *Cell Physiol Biochem* 41(4):1633–1648
14. Uthaisar K, Seubwai W, Srikoon P, Vaeteewoottacharn K, Sawanyawisuth K, Okada S, Wongkham S (2012) Cepharanthine suppresses metastatic potential of human cholangiocarcinoma cell lines. *Asian Pac J Cancer Prev* 13 Suppl:149–154
15. Li G, Qiao K, Xu X, Wang C (2022) Cepharanthine Regulates Autophagy via Activating the p38 Signaling Pathway in Lung Adenocarcinoma Cells. *Anticancer Agents Med Chem* 22(8):1523–1529
16. Hopkins AL (2008) Network pharmacology: the next paradigm in drug discovery. *Nat Chem Biol* 4(11):682–690

17. Ru J, Li P, Wang J, Zhou W, Li B, Huang C, Li P, Guo Z, Tao W, Yang Y, Xu X, Li Y, Wang Y, Yang L (2014) TCMSP: a database of systems pharmacology for drug discovery from herbal medicines. *J Cheminform* 6:13
18. Daina A, Michielin O, Zoete V (2019) SwissTargetPrediction: updated data and new features for efficient prediction of protein targets of small molecules. *Nucleic Acids Res* 47(W1):W357–W364
19. Wang X, Shen Y, Wang S, Li S, Zhang W, Liu X, Lai L, Pei J, Li H (2017) PharmMapper 2017 update: a web server for potential drug target identification with a comprehensive target pharmacophore database. *Nucleic Acids Res* 45(W1):W356–W360
20. Ritchie ME, Phipson B, Wu D, Hu Y, Law CW, Shi W, Smyth GK (2015) limma powers differential expression analyses for RNA-sequencing and microarray studies. *Nucleic Acids Res* 43(7):e47
21. Shannon P, Markiel A, Ozier O, Baliga NS, Wang JT, Ramage D, Amin N, Schwikowski B, Ideker T (2003) Cytoscape: a software environment for integrated models of biomolecular interaction networks. *Genome Res* 13(11):2498–2504
22. Yu G, Wang LG, Han Y, He QY (2012) clusterProfiler: an R package for comparing biological themes among gene clusters. *OMICS* 16(5):284–287
23. Morris GM, Huey R, Lindstrom W, Sanner MF, Belew RK, Goodsell DS, Olson AJ (2009) AutoDock4 and AutoDockTools4: Automated docking with selective receptor flexibility. *J Comput Chem* 30(16):2785–2791
24. Trott O, Olson AJ (2010) AutoDock Vina: improving the speed and accuracy of docking with a new scoring function, efficient optimization, and multithreading. *J Comput Chem* 31(2):455–461
25. Malta TM, Sokolov A, Gentles AJ, Burzykowski T, Poisson L, Weinstein JN, Kaminska B, Huelsken J, Omberg L, Gevaert O, Colaprico A, Czerwinska P, Mazurek S, Mishra L, Heyn H, Krasnitz A, Godwin AK, Lazar AJ, Stuart JM, Hoadley KA, Laird PW, Noushmehr H, Wiznerowicz M (2018) Machine Learning Identifies Stemness Features Associated with Oncogenic Dedifferentiation. *Cell* 173(2):338–354e315
26. Newman AM, Liu CL, Green MR, Gentles AJ, Feng W, Xu Y, Hoang CD, Diehn M, Alizadeh AA (2015) Robust enumeration of cell subsets from tissue expression profiles. *Nat Methods* 12(5):453–457
27. Ru B, Wong CN, Tong Y, Zhong JY, Zhong SSW, Wu WC, Chu KC, Wong CY, Lau CY, Chen I, Chan NW, Zhang J (2019) TISIDB: an integrated repository portal for tumor-immune system interactions. *Bioinformatics* 35(20):4200–4202
28. Grabauskiene S, Bergeron EJ, Chen G, Thomas DG, Giordano TJ, Beer DG, Morgan MA, Reddy RM (2014) Checkpoint kinase 1 protein expression indicates sensitization to therapy by checkpoint kinase 1 inhibition in non-small cell lung cancer. *J Surg Res* 187(1):6–13
29. Zhou W, Wang Y, Lu A, Zhang G (2016) Systems Pharmacology in Small Molecular Drug Discovery. *Int J Mol Sci* 17(2):246
30. Saikia S, Bordoloi M (2019) Molecular Docking: Challenges, Advances and its Use in Drug Discovery Perspective. *Curr Drug Targets* 20(5):501–521
31. Kikukawa Y, Okuno Y, Tatetsu H, Nakamura M, Harada N, Ueno S, Kamizaki Y, Mitsuya H, Hata H (2008) Induction of cell cycle arrest and apoptosis in myeloma cells by cepharanthine, a

- biscoclaurine alkaloid. *Int J Oncol* 33(4):807–814
32. Chen Z, Huang C, Yang YL, Ding Y, Ou-Yang HQ, Zhang YY, Xu M (2012) Inhibition of the STAT3 signaling pathway is involved in the antitumor activity of cepharanthine in SaOS2 cells. *Acta Pharmacol Sin* 33(1):101–108
  33. Wang Y, Su GF, Huang ZX, Wang ZG, Zhou PJ, Fan JL, Wang YF (2020) Cepharanthine hydrochloride induces mitophagy targeting GPR30 in hepatocellular carcinoma (HCC). *Expert Opin Ther Targets* 24(4):389–402
  34. Shahriyar SA, Woo SM, Seo SU, Min KJ, Kwon TK (2018) Cepharanthine Enhances TRAIL-Mediated Apoptosis Through STAMBPL1-Mediated Downregulation of Survivin Expression in Renal Carcinoma Cells. *Int J Mol Sci* 19 (10)
  35. Liu Y, Xie Y, Lin Y, Xu Q, Huang Y, Peng M, Lai W, Zheng Y (2020) Cepharanthine as a Potential Novel Tumor-Regional Therapy in Treating Cutaneous Melanoma: Altering the Expression of Cathepsin B, Tumor Suppressor Genes and Autophagy-Related Proteins. *Front Bioeng Biotechnol* 8:601969
  36. Zhang X, Zhang G, Zhao Z, Xiu R, Jia J, Chen P, Liu Y, Wang Y, Yi J (2021) Cepharanthine, a novel selective ANO1 inhibitor with potential for lung adenocarcinoma therapy. *Biochim Biophys Acta Mol Cell Res* 1868(12):119132
  37. Bjerkvig R, Tysnes BB, Aboody KS, Najbauer J, Terzis AJ (2005) Opinion: the origin of the cancer stem cell: current controversies and new insights. *Nat Rev Cancer* 5(11):899–904
  38. Miranda A, Hamilton PT, Zhang AW, Pattnaik S, Becht E, Mezheyeuski A, Bruun J, Micke P, de Reynies A, Nelson BH (2019) Cancer stemness, intratumoral heterogeneity, and immune response across cancers. *Proc Natl Acad Sci U S A* 116(18):9020–9029
  39. Shibue T, Weinberg RA (2017) EMT, CSCs, and drug resistance: the mechanistic link and clinical implications. *Nat Rev Clin Oncol* 14(10):611–629
  40. Blokzijl F, de Ligt J, Jager M, Sasselli V, Roerink S, Sasaki N, Huch M, Boymans S, Kuijk E, Prins P, Nijman IJ, Martincorena I, Mokry M, Wiegerinck CL, Middendorp S, Sato T, Schwank G, Nieuwenhuis EE, Verstegen MM, van der Laan LJ, de Jonge J, Ijzermans JN, Vries RG, van de Wetering M, Stratton MR, Clevers H, Cuppen E, van Boxtel R (2016) Tissue-specific mutation accumulation in human adult stem cells during life. *Nature* 538(7624):260–264

## Tables

Table 1  
The result of the lowest binding affinity of molecular docking.

Target name	Uniprot ID	PDB ID	Binding affinity (kcal/mol)
AURKA	O14965	1mq4	-9.1
CCNA2	P20248	1fin	-8.4
CCNE1	P24864	1w98	-9.0
CDK1	P06493	4y72	-9.2
CHEK1	O14757	1ia8	-7.6
PLK1	P53350	1q4o	-8.5

## Figures

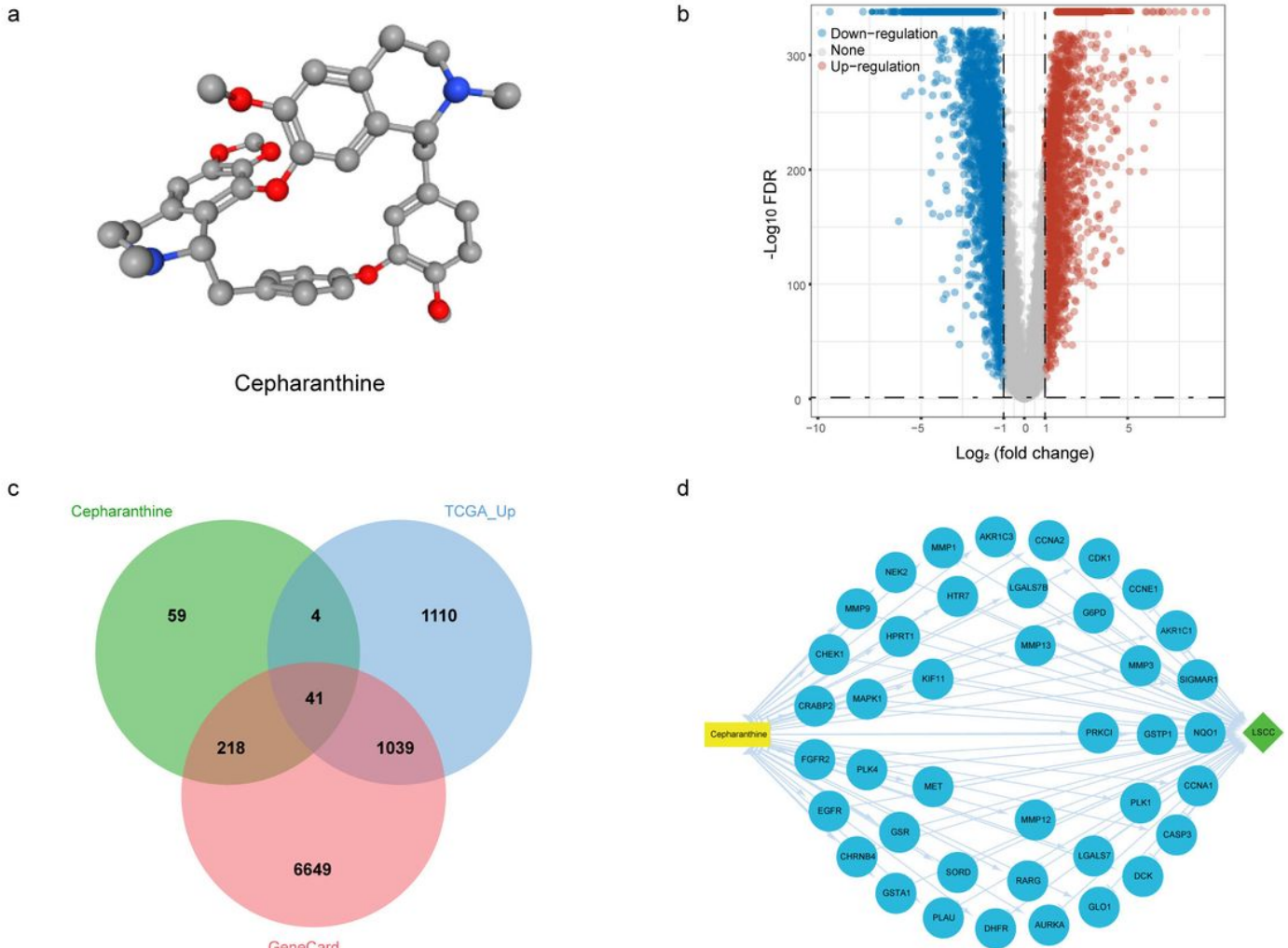


## Figure 1

Common targets of CEP and LUSC. (a) 3D structure of CEP. (b) Volcano plot of differentially expressed genes. (c) Venn diagram of intersecting targets. (d) drug-target-disease network

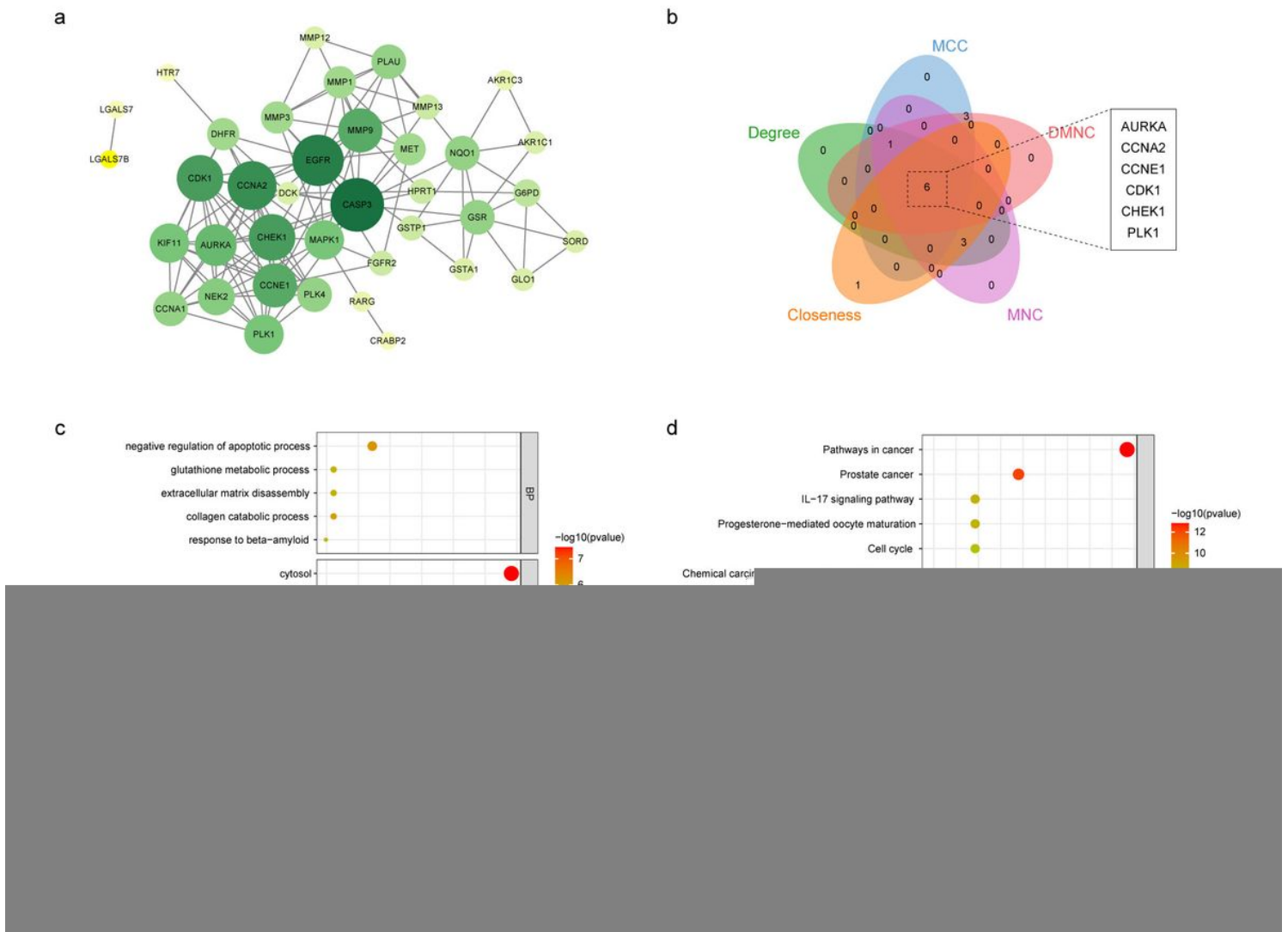


## Figure 2

Interaction and enrichment analysis of target proteins. (a) The visualizing interaction network of target proteins. (b) Topological screening of hub genes. (c) GO enrichment analysis. (d) KEGG pathway enrichment analysis

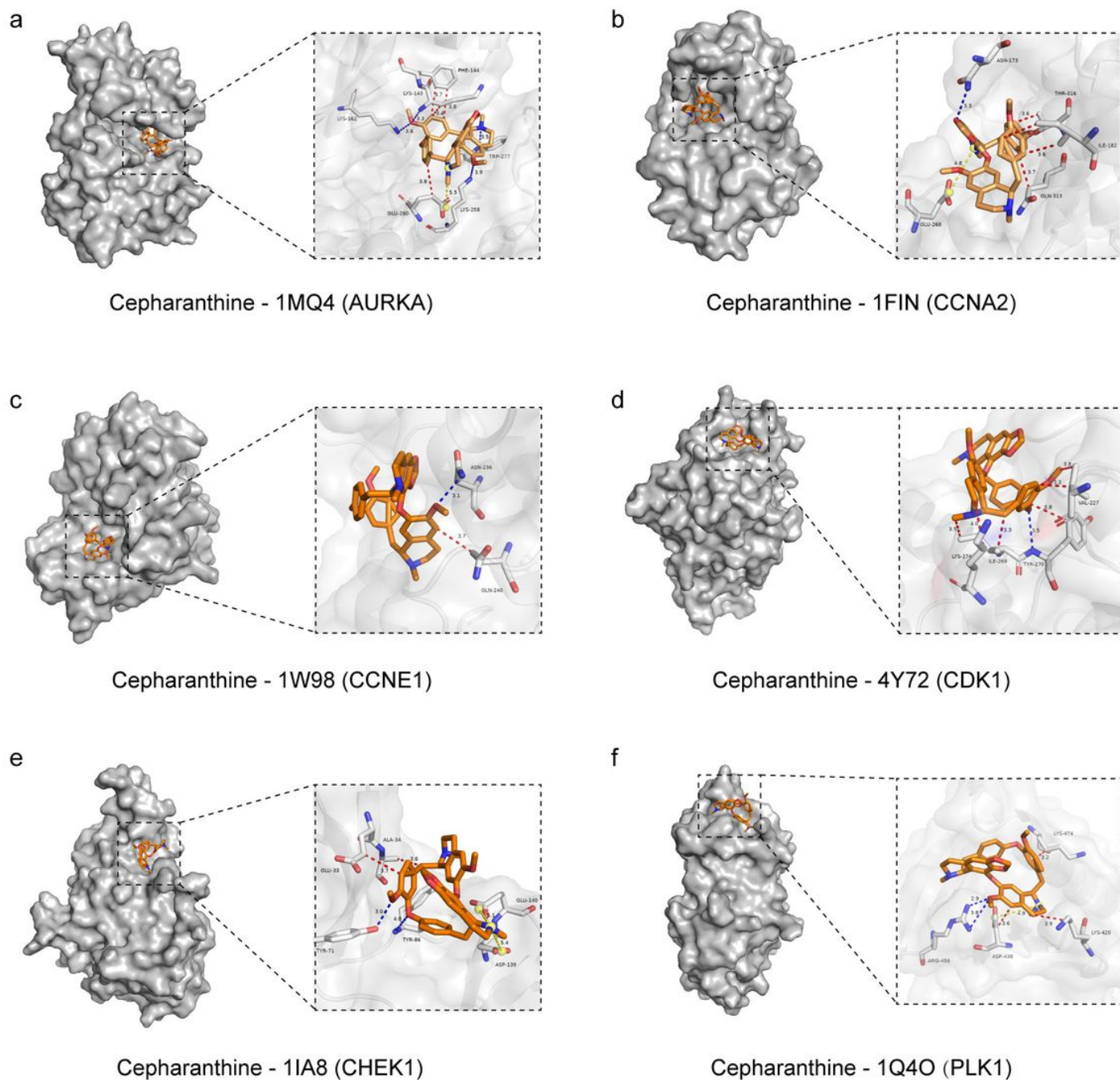


**Figure 3**

Molecular docking. (a) Docking of CEP and AURKA. (b) Docking of CEP and CCNA2. (c) Docking of CEP and CCNE1. (d) Docking of CEP and CDK1. (e) Docking of CEP and CHEK1. (f) Docking of CEP and PLK1. Dashed blue lines represent hydrogen bonds, dashed red lines represent hydrophobic interactions, and solid red lines represent salt bridge

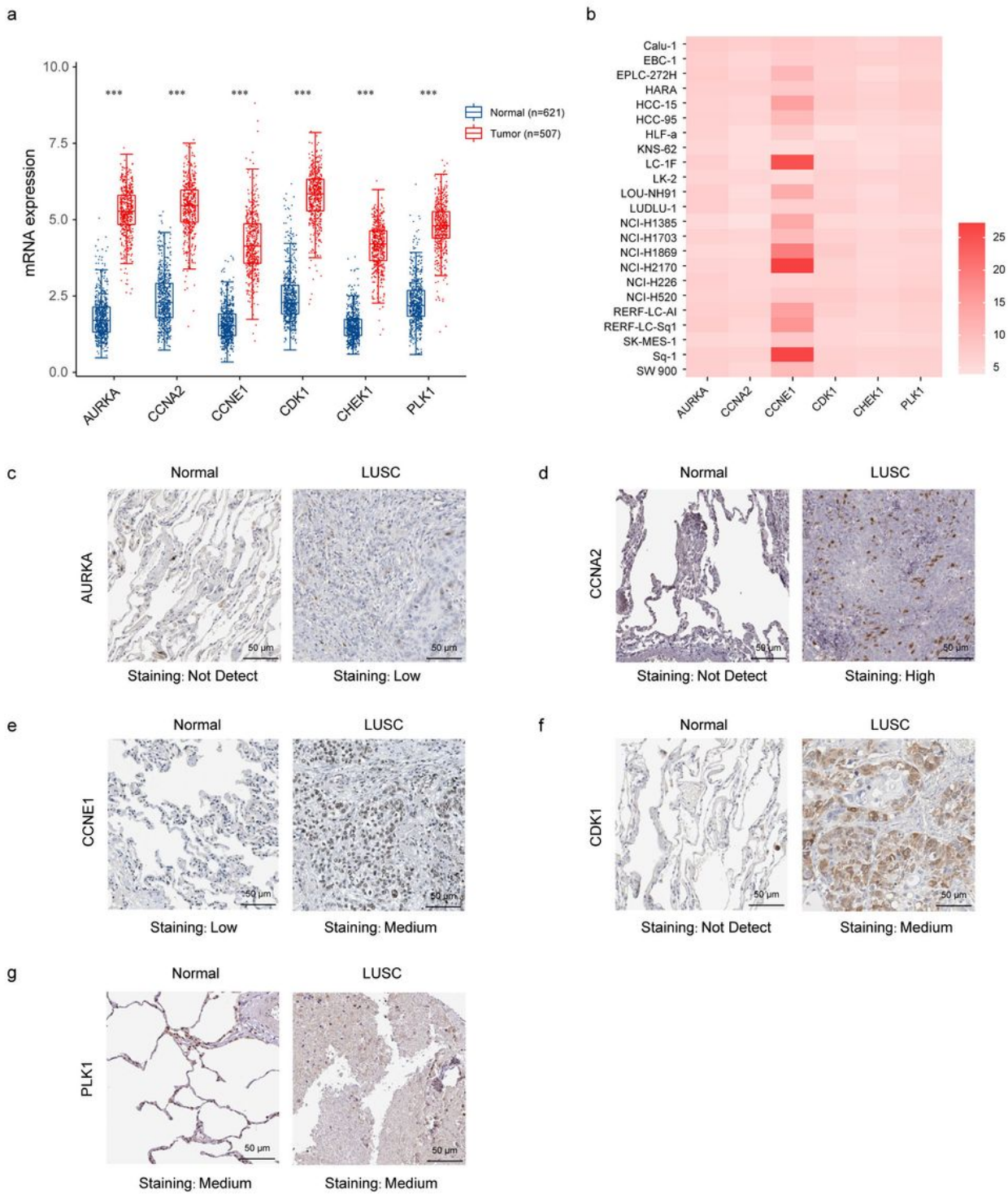


**Figure 4**

Expression of these targets. (a) Transcriptional expression of targets from TCGA. (b) Expressed differently of targets in various cell lines. (c-g) Protein expression of targets in HPA.

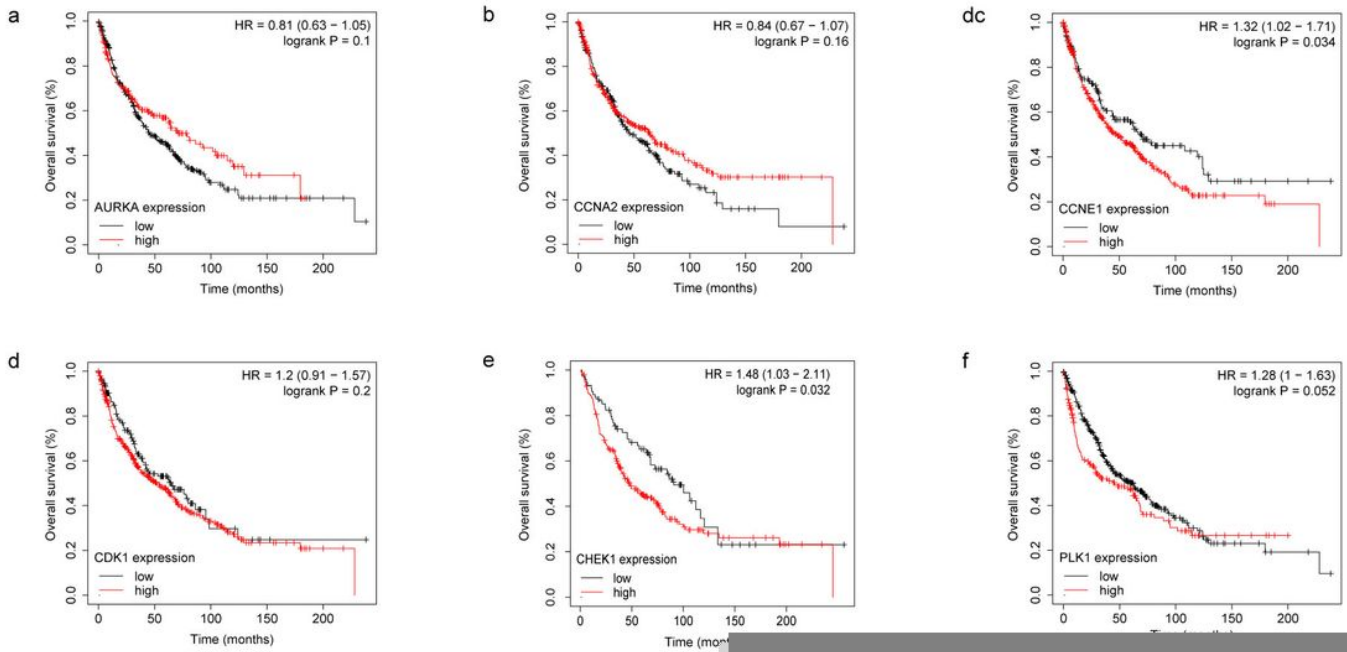


**Figure 5**

Overall survival. Comparison of overall survival between the different expression level of AURKA (a), CCNA2 (b), CCNE1 (c), CDK1 (d), CHEK1 (e) and PLK1 (f)

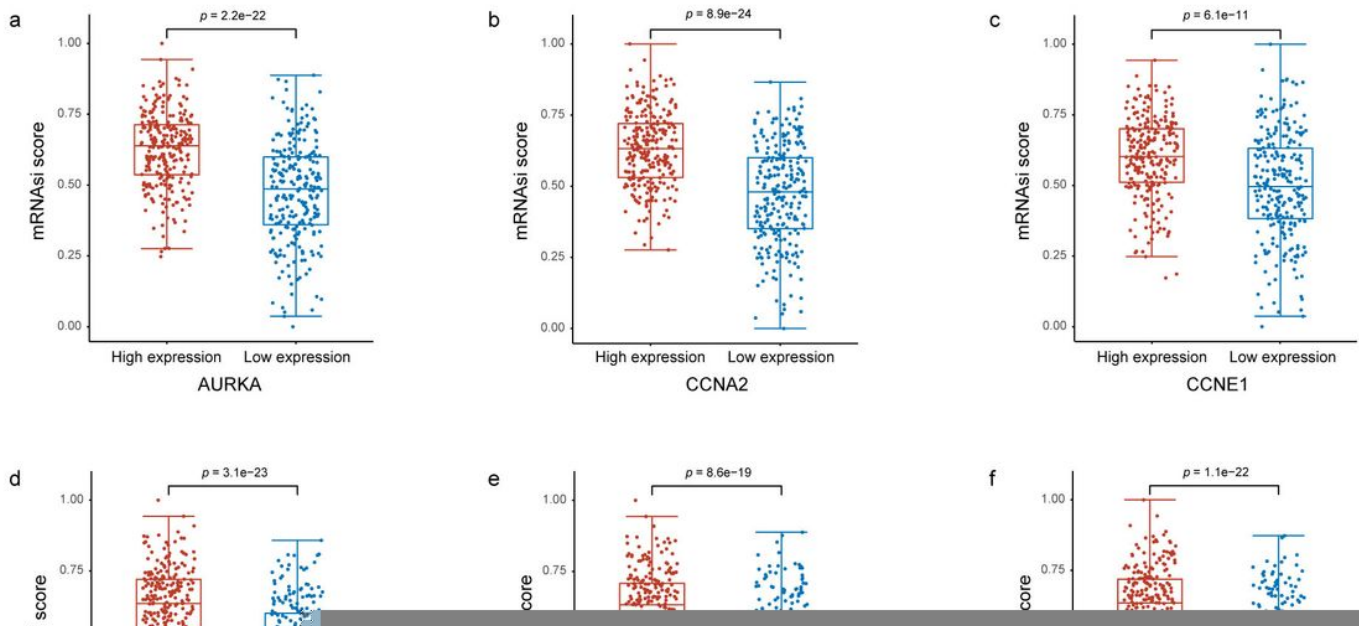


**Figure 6**

Cancer stemness index. Analysis of mRNA differences in samples with different expression levels of AURKA (a), CCNA2 (b), CCNE1 (c), CDK1 (d), CHEK1 (e) and PLK1 (f)

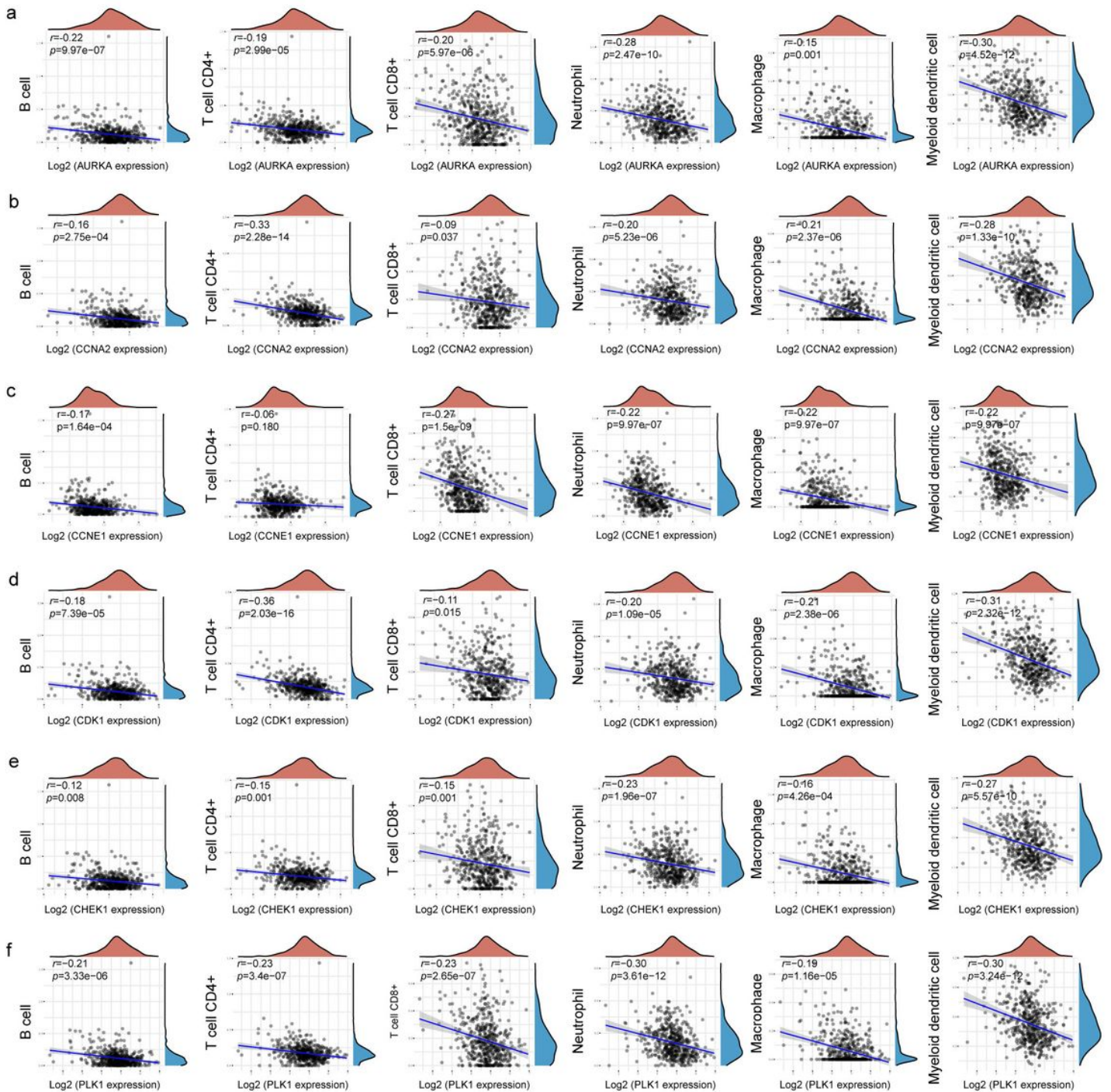


**Figure 7**

Immune cell infiltration. Correlation between expression level of AURKA (a), CCNA2 (b), CCNE1 (c), CDK1 (d), CHEK1 (e) and PLK1 (f) and immune cell infiltration

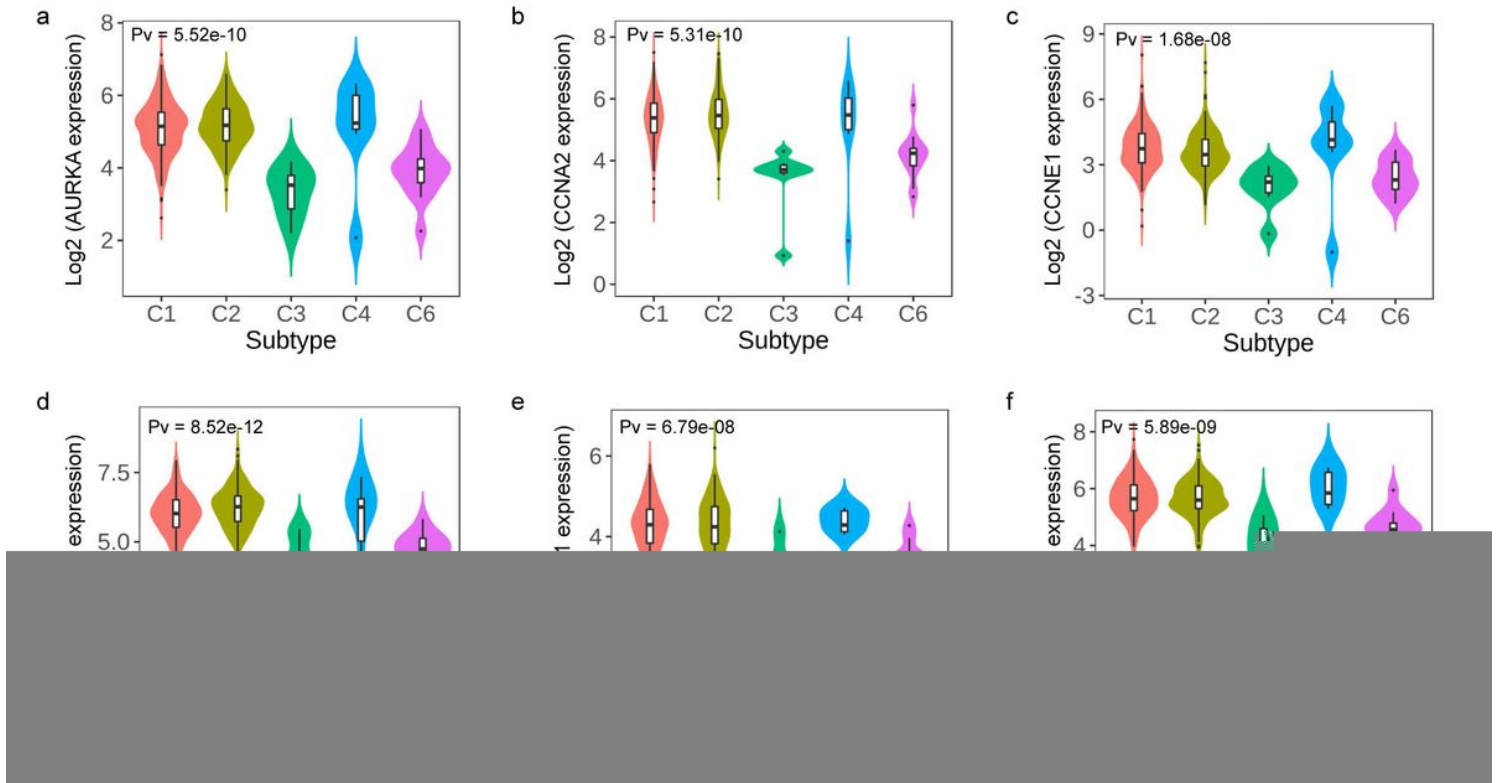


**Figure 8**

Immune subtypes of LUSC. The relationship between expression of AURKA (a), CCNA2 (b), CCNE1 (c), CDK1 (d), CHEK1 (e) and PLK1 (f) and immune subtypes. C1, wound healing. C2, IFN-gamma dominant. C3, inflammatory. C4, lymphocyte depleted. C5, immunologically quiet. C6, TGF- $\beta$  dominant

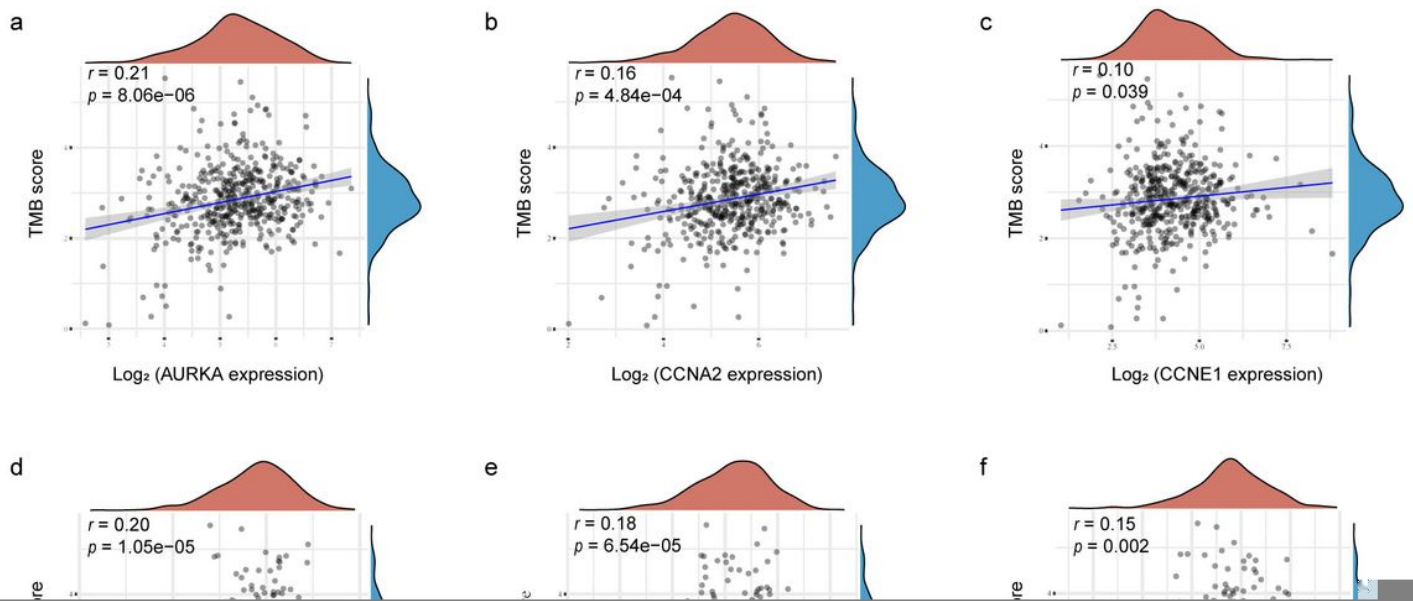


**Figure 9**

Tumor mutation burden. The relationship between expression of AURKA (a), CCNA2 (b), CCNE1 (c), CDK1 (d), CHEK1 (e) and PLK1 (f) and tumor mutation burden.

## Supplementary Files

This is a list of supplementary files associated with this preprint. Click to download.

- [TableS1.docx](#)
- [TableS2.docx](#)
- [TableS3.docx](#)
- [TableS4bindingsite.docx](#)